

Isolation and Anti-HIV-1 Integrase Activity of Lentzeosides A-F from Extremotolerant

Lentzea sp. H45, a strain isolated from a high altitude Atacama Desert soil

Running head: Lentzeosides A-F from Extremotolerant *Lentzea* sp. H45

Dominik Wichner,^{1,9} Hamidah Idris,² Wael E. Houssen,^{1,4,8} Andrew R. McEwan,^{1,4} Alan T. Bull,⁵
Juan A. Asenjo,⁷ Michael Goodfellow,² Marcel Jaspars,¹ Rainer Ebel,¹ and Mostafa E. Rateb,^{1,3,6,*}

¹ Marine Biodiscovery Centre, University of Aberdeen, Aberdeen AB24 3UE, Scotland, UK.

² School of Biology, Newcastle University, Newcastle upon Tyne NE1 7RU, UK.

³ School of Science & Sport, University of the West of Scotland, Paisley PA1 2BE, UK.

⁴ Institute of Medical Sciences, University of Aberdeen, Aberdeen AB25 2ZD, Scotland, UK.

⁵ School of Biosciences, University of Kent, Canterbury, Kent CT2 7NJ, U.K.

⁶ Pharmacognosy Department, School of Pharmacy, Beni-Suef University, Beni-Suef 32514, Egypt.

⁷ Centre for Biotechnology and Bioengineering (CeBiB), Department of Chemical Engineering and Biotechnology, Universidad de Chile, Beauchef 851, Santiago 8370450, Chile.

⁸ Pharmacognosy Department, Faculty of Pharmacy, Mansoura University, Mansoura 35516, Egypt.

⁹ University of Regensburg, Universitätsstraße 31, Regensburg 93053, Germany.

The extremotolerant isolate H45 was one of several actinomycetes isolated from a high altitude Atacama Desert soil collected in northwest Chile. The isolate was identified as a new *Lentzea* sp. using a combination of chemotaxonomic, morphological and phylogenetic properties. Large scale fermentation of the strain in two different media followed by chromatographic purification led to the isolation of six new diene and monoene glycosides named lentzeosides A–F, together with the known compound (Z)-3-hexenyl glucoside. The structures of the new compounds were confirmed by HRESIMS and NMR analyses. Compounds **1-6** displayed moderate inhibitory activity against HIV integrase.

* **Correspondence:** Mostafa E. Rateb, E-mail: mostafa.rateb@uws.ac.uk, Tel: +4414418483072

INTRODUCTION

Natural products are known to be a rich source of diverse chemical scaffolds for drug discovery. However, their use has diminished in the past two decades, mainly due to technical barriers when screening natural products in high-throughput assays against molecular targets and to their limited availability for clinical trials.¹ Additionally, the discovery of new bioactive natural products is challenging due to the high rate of re-discovery of known metabolites, a problem that can be addressed by isolating and screening novel microorganisms from underexplored habitats, such as desert biomes^{2,3}, and by incorporating rigorous dereplication procedures into all stages of the discovery process. In addition, industry has realized that phenotypic screening is more effective at discovering new bioactive compounds than narrow screening of molecular targets.

The Atacama Desert in Chile is known for its extreme aridity which has persisted for at least ~15 million years.⁴ Some regions in the desert were once thought to have “Mars-like” soils deemed too extreme for life to exist given high levels of UV radiation, the presence of inorganic oxidants, areas of high salinity, and very low concentrations of organic carbon.⁵ However, recent research has revealed extraordinary bacterial diversity across a range of Atacama environments^{6,7}, and many novel actinomycetes have been isolated from hyper – and extreme hyper-arid soils.^{8,9} Biological and genome-guided screening of some of these actinomycetes has led to the isolation and characterization of new natural products belonging to diverse structural classes and exhibiting various biological activities, as exemplified by the antimicrobial chaxamycins and chaxalactins isolated from *Streptomyces leeuwenhoekii* C34^T, the abenquines from *Streptomyces* sp. DB634, the antitumor atacamycins from *Streptomyces* sp. C38, and the cell invasion inhibitor chaxapeptin from *S. leeuwenhoekii* strain C58.¹⁰⁻¹⁶

As part of our ongoing program to investigate the extremobiosphere as a source of new natural products, we have focused our attention on *Lentzea* sp. strain H45 which was isolated from a high altitude Atacama Desert soil and shown to produce a specific pattern of secondary metabolites based on its LCMS profile and associated NMR data. Chemical screening of the strain on two different cultivation media led to the isolation of six new and one known diene, as well as monoene glycosides (Figure 1). Structure elucidation of these compounds was based on HRESIMS, 1D and 2D NMR analyses. The isolated compounds were screened for their inhibitory activity against HIV-1 integrase, an enzyme that is critical for the integration of the HIV genome into the host genome.¹⁷ This target is very attractive for the development of new anti-HIV therapy as it is selective for the virus.

RESULTS

In this study, actinobacterial isolate H45 was obtained from subsurface soil sample collected at an altitude > 5000 m in the vicinity of the ALMA Observatory in the Atacama Desert, Chile. The chemotaxonomic, morphological, physiological and phylogenetic properties of strain H45 are in line with its classification in the genus *Lentzea*.^{18,19} The strain was found to be an aerobic, Gram-positive actinomycete that formed a branched substrate mycelium and aerial hyphae that fragmented into rod-shaped elements (Figure 2), while chemical analysis of whole-organism hydrolysates revealed the presence of *meso*-diaminopimelic acid and galactose, mannose and ribose, and the predominant isoprenologue was tetrahydrogenated menaquinone with nine isoprene units (MK9[H4]). The organism formed a distinct branch at the periphery of the *Lentzea* 16S rRNA gene tree, a position that was supported by all of the tree-making algorithms and by a 69% bootstrap value (Figure 3). The strain was most closely, albeit loosely, related to *Lentzea kentuckyensis*^T

NRRL B-34416. These results clearly show that the isolate forms a new centre of taxonomic variation in the genus *Lentzea* consistent with its recognition as a putative new species.

Large scale fermentation of *Lentzea* sp. strain H45 on two different media supplemented with Diaion HP-20 resin was followed by methanolic extraction of the resin beads; subsequently, the crude extract was subject to multiple steps of medium and high pressure preparative C-18 chromatography which resulted in the isolation of six new and one known natural product based on HRESIMS and NMR data (Figure 1).

HRESIMS analysis of compound **1** yielded a $[M+Na]^+$ ion at m/z 281.1351 indicating a molecular formula of $C_{13}H_{22}O_5$. The analysis of 1H , ^{13}C and multiplicity-edited HSQC NMR spectra revealed the presence of one methylene (δ_C/δ_H 20.5/2.16) and one oxymethylene group (δ_C/δ_H 68.3/4.26, 4.08), one methyl doublet (δ_C/δ_H 17.9/1.15), one methyl triplet (δ_C/δ_H 14.2/0.94), four olefinic resonances (δ_C/δ_H 133.7/5.42, 129.6/5.71, 127.4/5.94, 127.0/6.58) and five oxymethine groups (δ_C/δ_H 102.1/4.15, 76.4/3.09, 75.3/2.80, 73.7/2.98, 71.5/3.15). Furthermore, the 1H NMR spectrum showed 3 hydroxy groups resonating at δ_H 4.8-5.1. The COSY correlations of H_2 -1 through H_3 -7 indicated a spin system comprising two conjugated olefins with a terminal ethyl group and established a (2*E*,4*Z*)-heptadien-1-ol substructure (Figure 4). This was corroborated by the HMBC correlations of H_2 -1/ C -3, H -2/ C -4, and H_3 -7 to both C -5 and C -6 (Figure 4). The COSY spectrum indicated a second spin system which included the signals H -1' to H_3 -6', which in combination with the HMBC correlation of H -1'/ C -5' suggested a β -L-quinovopyranose (β -L-6-deoxyglucopyranose), which was confirmed by the optical rotation, the coupling constant of the anomeric proton ($J = 7.8$ Hz), axial-axial proton couplings for H_1'/H_2' , H_2'/H_3' , H_3'/H_4' , H_4'/H_5' (Table 2) as well as the agreement of the ^{13}C NMR data and the ROESY correlations with reported data.²⁰ The sugar moiety was further confirmed by acid hydrolysis of **1** upon which α -L-quinovose

was detected by co-chromatography on TLC in comparison with authentic sugar samples. Finally, the connectivity of the two substructures was confirmed by the HMBC correlation of H-1'/C-1. The geometry of the two double bonds was established as (2*E*,4*Z*) based on coupling constant data of H-2 and H-5 with values of 16.1 Hz and 10.1 Hz, respectively which was further supported by ROESY correlations of H-2/H-4, H-3/H₂-1, H-4/H-5 and H-3/H₂-6 (Figure 4). Based on this evidence, **1** was identified as a new natural product for which the name lentzeoside A is proposed.

Compound **2** shared the chemical formula with **1** as C₁₃H₂₂O₅ based on the HRESIMS analysis that gave an [M+Na]⁺ ion at *m/z* 281.1351. Comparison of the ¹H and ¹³C NMR data of **2** with those obtained for **1** revealed that **2** was the 1'-epimer of **1**, and the presence of an α-L-rhamnopyranose was corroborated by the optical rotation, the very small coupling of the anomeric proton and the agreement of the ¹³C NMR data and the ROESY correlations with the reported data.²¹ The sugar moiety was further confirmed by acid hydrolysis of **2** upon which α-L-rhamnose was detected by co-chromatography on TLC in comparison with authentic sugar samples. Thus, compound **2** was identified as a new secondary metabolite for which we propose the name lentzeoside B.

The molecular formula C₁₃H₂₂O₆ for compound **3** was established on the basis of HRESIMS analysis that afforded an [M+Na]⁺ ion at *m/z* 297.1299 indicating one more oxygen atom than in **1**. The ¹H, ¹³C NMR and multiplicity-edited HSQC spectra showed a close similarity to those obtained for **1**, but indicated that the β-L-rhamnopyranose unit in **1** had been replaced by a β-D-glucopyranose. This assumption was confirmed by the optical rotation, the magnitude of the coupling constant analysis of the anomeric proton (*J*=7.9 Hz) as well as the agreement of the ¹³C NMR data and the ROESY correlations with the reported data.²² The sugar moiety was further confirmed by acid hydrolysis of **3** upon which β-D-glucose was detected by co-chromatography

on TLC in comparison with authentic sugar samples. Therefore, the structure of **3** was established as depicted, representing a new natural product for which the name lentzeoside C is proposed.

The HRESIMS analysis of compound **4** provided a $[M+Na]^+$ ion at m/z 281.1349 indicating it to be an isomer of **2**. Analysis of the NMR spectra and the optical rotation indicated that the two compounds contained a α -L-rhamnopyranose, but differed in the geometry of the diene moiety. The coupling constant data of H-2 and H-5 with values of 16.1 Hz and 15.5 Hz, respectively indicated *E*-configurations for both olefinic groups in **4**. This was further supported by the ROESY correlations of H₂-1/H-3, H-3/H-5, H-2/H-4 and H-4/H₂-6 (Figure 4). On that basis, **4** was identified as a new secondary metabolite for which the name lentzeoside D is proposed.

The molecular formula of compounds **5** and **6** was deduced as C₁₂H₂₂O₅ as HRESIMS analysis of $[M+Na]^+$ and $[M+H]^+$ ions at m/z 269.1351 and 247.1545, respectively indicating one carbon atom less than **1**. NMR analysis and optical rotation of **5** and **6** indicated that they contained an α -L-rhamnopyranose and a β -L-quinovopyranose as described above for **2** and **1**, respectively, which was connected to the same (*Z*)-3-hexenyl side chain. The presence of the latter was evident from COSY correlations of H₂-1 through H₃-6. As the signals for H-3 and H-4 exhibited non-first order coupling, the *E*-configuration of the double bond was established based on ROESY correlations of H₂-1/H-3, H-4/H₃-6 and H₂-2/H₂-5 (Figure 4). Based on this information, compounds **5** and **6** were identified as new natural products for which the names lentzeoside E and F, respectively, are proposed.

Based on the NMR and accurate mass analyses, compound **7** was identified as (*Z*)-3-hexenyl glucoside, this compound has been isolated from several plant sources, such as *Epimedium grandiflorum*.²³

Compounds **1-6** were evaluated for their anti-HIV integrase activity at different concentrations. Compounds **3, 4** and **5** inhibited HIV integrase with IC₅₀ values of 21 µM, 16 µM and 21 µM respectively. Compounds **1, 2** and **6** were only weakly active, they did not give 50 % inhibition of the enzyme activity up to a concentration of 100 µM.

DISCUSSION

A major draw of filamentous actinomycetes, especially streptomycetes, is their unrivalled capacity to synthesize structurally diverse bioactive metabolites. In this context, the present study provides further evidence that taxonomically novel actinomycetes isolated from Atacama Desert soils are a rich source of new chemical entities. It is especially interesting that the new compounds, lentzosides A-F, are derived from a novel *Lentzia* strain as previously new specialized metabolites from Atacama Desert actinomycetes have come from novel *Streptomyces* strains,⁷ notably from a deep seated 16S rRNA gene clade that can be equated with the species, *Streptomyces leeuwenhoekii*.¹⁰⁻¹⁶ The genus *Lentzia* was validly published in 1995,²⁴ but to date does not appear to have been studied in terms of its natural product chemistry, though *Lentzia* sp. 7887 effects the biotransformation of FR901459, a novel derivative of cyclosporin.²⁵

Chemical screening of this novel *Lentzia* sp. strain H45 on two different media led to the isolation of six new diene and monoene glycosides and the known compound (Z)-3-hexenyl glucoside. It is interesting to note that this class of metabolites was not traced before from microbial sources and the most closely related known compound **7** which was also encountered in the present study had previously been obtained from plant sources. Due to the close similarity of lentzeosides, it could be argued that they were artifacts rather than natural products. To preclude this assumption and confirm them as natural products, they were directly detected by LCMS analysis of the fresh

bacterial culture broth before the inclusion of the Diaion HP20, extraction and purification process with the exact retention times, UV absorption and accurate mass.

Compounds **1-6** were found to inhibit HIV-1 integrase *in vitro*. Treatment of HIV usually involves a combination therapy of different drugs that target different stages of the viral replication cycle, a procedure that overcomes the development of resistance in the virus due to its high mutation rate²⁶. HIV integrase is one of the key enzymes in the virus replication cycle as it is responsible for the integration of the reverse transcribed viral cDNA into the host cell genome.²⁷ Raltegravir® is the first FDA clinically approved HIV integrase inhibitor used to treat both HIV-1 infections in treatment-experienced adult patients who have evidence of viral replication and HIV-1 strains resistant to multiple antiretroviral agents.²⁸

EXPERIMENTAL PROCEDURES

General Experimental Procedures. NMR data were acquired on a Varian VNMRS 600 MHz NMR spectrometer and LC-HRESIMS data obtained by using a LTQ/XL Orbitrap coupled to the HPLC system (PDA detector, PDA autosampler, and pump) under the following conditions: capillary voltage of 45 V, capillary temperature of 260 °C, auxiliary gas flow rate of 10–20 arbitrary units, sheath gas flow rate of 40–50 arbitrary units, spray voltage of 4.5 kV with a mass range of 100–2000 amu (maximal resolution of 30000). For LC/MS, a C18 analytical HPLC column (5 µm, 4.6 mm × 150 mm) was used with a mobile phase of 0 to 100% MeOH over 30 min at a flow rate of 1 mL.min⁻¹. Optical rotations were recorded using a Bellingham + Stanley ADP410 polarimeter. Medium Pressure Liquid Chromatographic separations were carried out using a Biotage SP1 flash system fitted with a reversed phase 40iM cartridge (KP-C18-HSTM, 40 x 150 mm), the detection was carried out at 220 and 254 nm. For RP-HPLC separations, a SunFire (C₁₈, 250 x 10 mm, 5 µm i.d.) column connected to an Agilent 1200 series binary pump was used and monitored with an

Agilent photodiode array detector, the detection was carried out at 220, 254, 280, and 320 nm. Acid hydrolysis of the isolated compounds was performed as reported before.²⁹ HPLC solvents and the authentic sugar samples were obtained from Sigma-Aldrich, the ingredients for fermentation were from Oxoid UK and Sigma-Aldrich and the Diaion HP-20 resin from Resindion S.R.L., a subsidiary of Mitsubishi Chemical Co., Binasco, Italy.

Microbial taxonomy and fermentation conditions. Strain H45 was isolated from a subsurface soil sample collected at 5048 meters above sea level on the Chajnantor plateau, in northeast Chile (23°00'48.8"S/67°45'30.8"W) by one of us (MG) in November 2012. The strain was isolated on Gauze's No. 1 agar³⁰ supplemented with the antifungal antibiotics cycloheximide and nystatin (each at 25 µg.mL⁻¹) using the procedure described by Okoro *et al.*⁸ The strain has phenotypic properties consistent with its classification in the genus *Lentzea* and forms a distinct phyletic line in the *Lentzea* 16S rRNA gene tree. The *Lentzea* isolate has been deposited in the NCIMB and NRRL public service collections under the accession numbers 14966 and B-65282 respectively, the GenBank accession number of the 16S rRNA gene sequence of the strain is LT009512. Two cultivation media were used for large scale fermentation of the strain: Medium 410 contained glucose (10.0 g), glycerol (10.0 g), casamino acids (15.0 g), oatmeal (5.0 g), peptone (10.0 g), yeast extract (5.0 g), CaCO₃ (1.0 g) and distilled water to 1 L, pH 7.0; and modified ISP2 medium malt extract (4.0 g), yeast extract (10.0 g), dextrose (10.0 g), glycerol (10.0 g), and distilled water to 1 L, pH 7.0. The strain was grown in 4 L of each of these media by shaking at 180 rpm in a shaker incubator at 30 °C for 7 days when HP-20 resin beads was added followed by shaking at 180 rpm for 6 h prior to centrifugation at 3000 rpm for 15 min.

Extraction and isolation. Biomass of the strain H45 and HP-20 resin beads were extracted with methanol (MeOH × 2) and acetone (×1) and the resultant extracts combined and concentrated *in*

1 *vacuo*. The combined extracts were purified using the Biotage flash system with a gradient of
 2 MeOH in water (5-100% in 12 column volumes). The eluted fractions of both media were screened
 3 using LCMS and ^1H NMR and the interesting fractions further purified using RP-HPLC. For
 4 medium 410, the second fraction was purified using a gradient of MeOH in $\text{H}_2\text{O}/\text{MeOH}$ (95:5)
 5 (25-100% in 25 min, flow rate 2.0 mL/min) to obtain compounds **1** (3.1 mg), **2** (1.0 mg), **3**
 6 (2.2 mg), **4** (1.0 mg), and **5** (2.0 mg). In the case of the modified ISP2 medium, the fourth fraction
 7 was purified using a gradient of MeOH in $\text{H}_2\text{O}/\text{MeOH}$ (95:5) (50-100% in 25 min, flow rate
 8 2.2 mL/min) to obtain compounds **1** (3.1 mg), **2** (1.1 mg), **5** (3.4 mg), **6** (3.4 mg), and **7** (2.2 mg).
 9 Lentzeoside A (**1**): Light yellow powder; $[\alpha]^{20}_{\text{D}} -25$ (c 0.15, MeOH); UV (MeOH) λ_{max} (log ϵ) at
 10 258 (3.2), 268 (3.6) and 280 (2.7) nm; ^1H and ^{13}C NMR data (Tables 1-2); HRESIMS m/z $[\text{M}+\text{Na}]^+$
 11 at 281.1351 indicting the molecular formula $\text{C}_{13}\text{H}_{22}\text{O}_5$ (calculated $[\text{M}+\text{Na}]^+$ ion at m/z 281.1359).
 12 Lentzeoside B (**2**): Light yellow powder; $[\alpha]^{20}_{\text{D}} -31$ (c 0.18, MeOH); UV (MeOH) λ_{max} (log ϵ) at
 13 258 (3.1), 270 (3.4) and 280 (2.5) nm; ^1H and ^{13}C NMR data (Tables 1-2); HRESIMS m/z $[\text{M}+\text{Na}]^+$
 14 at 281.1351 indicting the molecular formula $\text{C}_{13}\text{H}_{22}\text{O}_5$ (calculated $[\text{M}+\text{Na}]^+$ ion at m/z 281.1359).
 15 Lentzeoside C (**3**): Light yellow powder; $[\alpha]^{20}_{\text{D}} +38$ (c 0.10, MeOH); UV (MeOH) λ_{max} (log ϵ) at
 16 258 (3.2), 274 (3.8) and 282 (2.9) nm; ^1H and ^{13}C NMR data (Tables 1-2); HRESIMS m/z $[\text{M}+\text{Na}]^+$
 17 at 297.1299 indicting the molecular formula $\text{C}_{13}\text{H}_{22}\text{O}_6$ (calculated $[\text{M}+\text{Na}]^+$ ion at m/z 297.1309).
 18 Lentzeoside D (**4**): Light yellow powder; $[\alpha]^{20}_{\text{D}} -22$ (c 0.18, MeOH); UV (MeOH) λ_{max} (log ϵ) at
 19 258 (3.1), 270 (3.4) and 280 (2.5) nm; ^1H and ^{13}C NMR data (Tables 1-2); HRESIMS m/z $[\text{M}+\text{Na}]^+$
 20 at 281.1349 indicting the molecular formula $\text{C}_{13}\text{H}_{22}\text{O}_5$ (calculated $[\text{M}+\text{Na}]^+$ ion at m/z 281.1359).

Lentzeoside E (**5**): colorless powder; $[\alpha]^{20}_D -29$ (c 0.15, MeOH); UV (MeOH) λ_{\max} (log ϵ) at 239 (3.6) nm; ^1H and ^{13}C NMR data (Tables 1-2); HRESIMS m/z $[\text{M}+\text{Na}]^+$ at 269.1351 indicting the molecular formula $\text{C}_{12}\text{H}_{22}\text{O}_5$ (calculated $[\text{M}+\text{Na}]^+$ ion at m/z 269.1359).

Lentzeoside F (**6**): colorless powder; $[\alpha]^{20}_D -25$ (c 0.18, MeOH); UV (MeOH) λ_{\max} (log ϵ) at 241 (3.4) nm; ^1H and ^{13}C NMR data (Tables 1-2); HRESIMS m/z $[\text{M}+\text{H}]^+$ at 247.1545 indicting the molecular formula $\text{C}_{12}\text{H}_{22}\text{O}_5$ (calculated $[\text{M}+\text{H}]^+$ ion at m/z 247.1540).

Anti-HIV-1 integrase activity. The HIV-1 integrase inhibitory activities of compounds 1-6 were evaluated using a kit purchased from XpressBio Life Science Products (Frederick, MD 21705, USA) and by following the manufacturer's protocol. Briefly, biotin-linked HIV-1 LTR U5 donor substrate (DS) DNA was applied to a streptavidin-coated 96-well plate, the test compounds were then added along with target substrate DNA and HIV integrase. The integrase processes the HIV-1 LTR U5 and catalyzes the strand transfer recombination reaction to integrate the DS DNA into the target substrate DNA. The products of these reactions were detected colorimetrically using an HRP-labeled antibody, sodium azide was used as a positive inhibitory control. Each compound was tested at 4 different concentrations (100, 50, 12.5 and 3.1 μM) in triplicate.

CONFLICT OF INTEREST

The authors declare no conflict of interest.

ACKNOWLEDGEMENTS

We thank the College of Physical Sciences, University of Aberdeen, for provision of infrastructure and facilities in the Marine Biodiscovery Centre, and staff at the European Southern Observatory for permission and assistance in collecting soil samples from the Chajnantor plateau. A.T.B and J.A.A thank The Royal Society for support (International Joint Project Grant JP 100654). JAA

1 thanks Conicyt for the Basal Grant FB0001 for the Centre CeBiB. H.I. is grateful for a scholarship
2 from the Malaysian Government and M.G. for an Emeritus Fellowship from the Leverhulme Trust.

3 REFERENCES

4 1 L. Harvey, A. L., Edrada-Ebel, R. & Quinn, R. J. The re-emergence of natural products for drug
5 discovery in the genomics era. *Nature Rev. Drug Discover.* **14**, 111–129 (2015).

6 2 Pidot, S. J.; Coyne, S.; Kloss, F.; Hertweck, C. Antibiotics from neglected bacterial sources. *Int.*
7 *J. Med. Microbiol.* **304**, 14–22 (2014).

8 3 Bull, A. T. Actinobacteria of the extremobiosphere. In *Extremophiles Handbook*; Horikoshi, K.,
9 Antranikian, G., Bull, A. T., Robb, F., Stetter, K., Eds.; Springer-Verlag: Tokyo, **2**, 1203–1240
10 (2011).

11 4 Gómez-Silva, B., Rainey, F. A., Warren-Rhodes, K. A., McKay, C. P. & Navarro-González, R.
12 Atacama Desert soil microbiology. In *Microbiology of Extreme Soils*, Soil Biology; Dion, P.,
13 Nautiyal, C. S., Eds.; Springer: Berlin, **13**, 117–132 (2008).

14 5 Navarro-González, R. *et al.* Mars-Like soils in the Atacama Desert, Chile, and the dry limit of
15 microbial Life. *Science* **302**, 1018–1021 (2003).

16 6. Crits-Christoph, A. *et al.* Colonization patterns of soil microbial communities in the Atacama
17 Desert. *Microbiome* **1**:28. DOI:10.1186/2049-2618-1-28 (2013).

18 7. Bull, A.T. *et al.* The Atacama Desert: technical resources and the growing importance of novel
19 microbial diversity. *Ann Rev Microbiol* **70**, in press (2016)

20 8 Okoro, C. K. *et al.* Diversity of culturable actinomycetes in hyper-arid soils of the Atacama
21 Desert, Chile. *Antonie van Leeuwenhoek* **95**, 121–133 (2009).

- 9 Bull, A. T. & Asenjo, J. A. Microbiology of hyper-arid environments: recent insights from the Atacama Desert, Chile. *Antonie van Leeuwenhoek* **103**, 1173–1179 (2013).
- 10 Rateb, M. E. *et al.* Chaxamycins A–D, bioactive ansamycins from a hyper-arid desert *Streptomyces* sp. *J. Nat. Prod.* **74**, 1491–1499 (2011).
- 11 Rateb, M. E. *et al.* Diverse metabolic profiles of a *Streptomyces* strain isolated from a hyper-arid environment. *J. Nat. Prod.* **74**, 1965–1971 (2011).
- 12 Schulz, D. *et al.* Abenquines A–D: aminoquinone derivatives produced by *Streptomyces* sp. strain DB634. *J. Antibiot.* **64**, 763–768 (2011).
- 13 Nachtigall, J. *et al.* Atacamycins A–C, 22-membered antitumor macrolactones produced by *Streptomyces* sp. C38. *J. Antibiot.* **64**, 775–780 (2011).
- 14 Elsayed, S. S. *et al.* Chaxapeptin, a lasso peptide from extremotolerant *Streptomyces leeuwenhoekii* strain C58 from the hyperarid Atacama Desert. *J. Org. Chem.* **80**, 10252–10260 (2015).
- 15 Busarakam, K. *et al.* *Streptomyces leeuwenhoekii* sp. nov., the producer of chaxalactins and chaxamycins, forms a distinct branch in *Streptomyces* gene trees. *Antonie van Leeuwenhoek* **105**, 849–861 (2014).
- 16 Gomez-Escribano J. P. *et al.* The *Streptomyces leeuwenhoekii* genome: *de novo* sequencing and assembly in single contigs of the chromosome, circular plasmid pSLE1 and linear plasmid pSLE2. *BMC Genomics* **16**, 485 (2015).
- 17 Craigie, R. HIV integrase, a brief overview from chemistry to therapeutics. *J. Biol. Chem.* **276**, 23213–23216 (2001) Craigie, R. The road to HIV-1 integrase inhibitors: the case for supporting basic research. *Future Virol* **9**, 899–903 (2014).

- 18 Labeda, D. P. Genus XI. *Lentzea* Yassin, Rainey, Brzezinka, Jahnke, Weissbrodt,
Budzikiewicz, Stackebrandt, and Schaal 1995, 362vp emend. Labeda, Hatano, Kroppenstedt and
Tamura 2001, 1049, in Goodfellow, M. *et al* (eds.) Bergey's Manual of Systematic Bacteriology.
2nd edn., Vol 5, The *Actinobacteria*, Part B, New York: Springer, pp 1379-1383 (2012).
- 19 Cao, C.-L. *et al.* *Lentzea guizhouensis* sp. nov., a novel lithophilous actinobacterium isolated
from limestone from the Karst area, Guizhou, China. *Antonie van Leeuwenhoek* **108**, 1365–1372
(2015).
- 20 Kiuchi, F. *et al.* Acacia concinna Saponins. II. Structure of monoterpenoid glycosides in the
alkaline hydrolysate of the saponin fraction. *Chem. Pharm. Bull.* **45**, 807–812 (1997).
- 21 Francis, J *et al.* Insulin Secretagogues from *Moringa oleifera* with cyclooxygenase enzyme and
lipid peroxidation inhibitory activities. *Helv. Chim. Acta.* **87**, 317–326 (2004).
- 22 Fujimoto, H. & Isomura, M. Chemical studies on chinese traditional medicine, Dangshen. I.
Isolation of (Z)-3- and (E)-2-hexenyl β -D-glucosides. *Biosci. Biotechnol. Biochem.* **36**, 2689–
2690 (1988).
- 23 Miyase, T. *et al.* Studies on the glycosides of *Epimedium grandiflorum* MORR. var.
thunbergianum (MIQ.) NAKAI. III. *Chem. Pharm. Bull.* **36**, 2475–2484 (1988).
- 24 Yassin, A. F. *et al.* *Lentzea* gen. nov., a new genus of the order *Actinomycetales*. *Int. J. Syst.*
Bacteriol. **45**, 357–363 (1995).
- 25 Sasamura, S. *et al.* Bioconversion of FR901459, a novel derivative of cyclosporin A, by *Lentzea*
sp. 7887. *J. Antibiot.* **68**, 511–520 (2015).
- 26 Maes, M., Loyter, A. & Friedler, A. Peptides that inhibit HIV-1 integrase by blocking its
protein–protein interactions, *FEBS Journal* **279**, 2795–2809 (2012).

27 Sherman, M. P. & Greene, W. C. Slipping through the door: HIV entry into the nucleus.

Microbes Infect **4**, 67–73 (2002).

28 Hicks, C. & Gulick, R. M. Raltegravir: the first HIV type 1 integrase inhibitor. *Clin Infect Dis*

48, 931–939 (2009).

29 Nakanishi, T., Inada, A., Kambayashi, K. & Yoneda, K. Flavonoid glycosides of the roots of

Glycyrrhiza uralensis. *Phytochem.* **24**, 339–341 (1985).

30 Zakharova, O. S., Zenova, G. M. & Zvyagintsev, D. G. Some approaches to the selective

isolation of actinomycetes of the Genus *Actinomadura* from soil. *Microbiology* **72**, 110–113

(2003).

Figure legends

Figure 1. Compounds isolated from *Lentzea* sp. H45.

Figure 2. Scanning electron micrograph of *Lentzea* sp. H45 showing fragmentation of aerial hyphae into rod-shaped elements following growth on ISP 3 agar after incubation at 28 °C for 10 days. Bar 1µm.

Figure 3. Neighbour-joining phylogenetic tree based on 16S rRNA gene sequences showing relationships between isolate H45 and the type strains of *Lentzea* and *Lechevalieria* species. Asterisks indicate branches of the tree that were also recovered using the maximum-likelihood and maximum-parsimony tree-making methods. Numbers at the nodes indicate levels of bootstrap support based on a neighbour-joining analysis of 1000 resampled datasets, only values above 50% are shown.

Figure 4. Key COSY, HMBC and ROESY correlations of compounds **1**, **4**, and **5**.

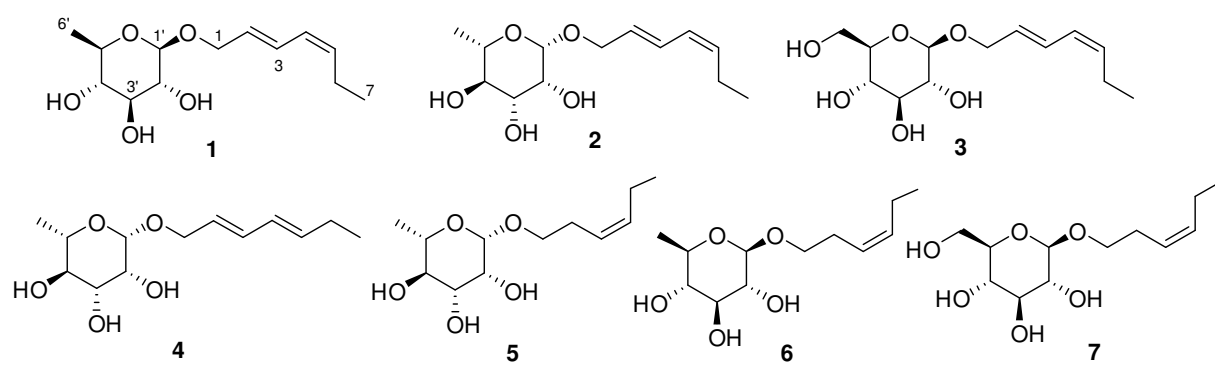


Figure 1. Compounds isolated from *Lentzea* sp. H45.

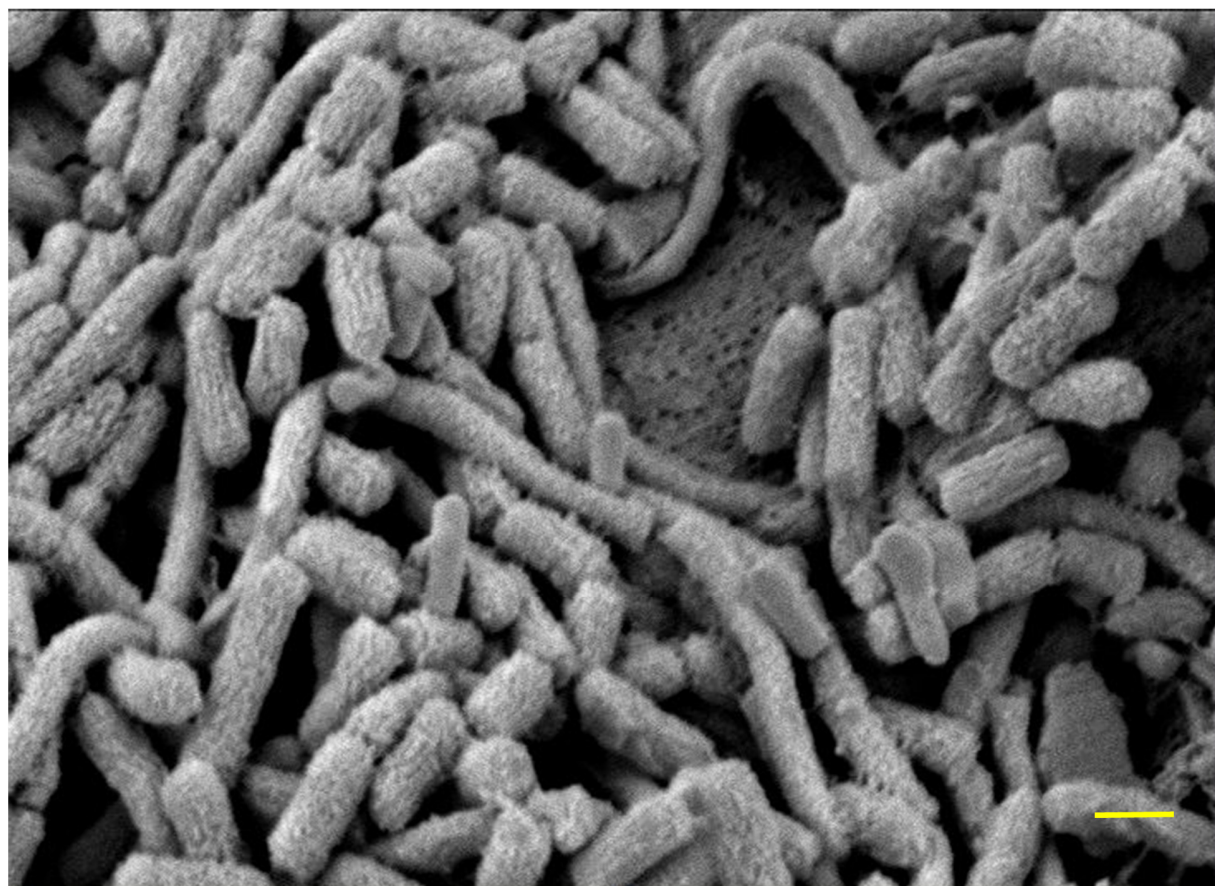


Figure 2. Scanning electron micrograph of *Lentzea* sp. H45 showing fragmentation of aerial hyphae into rod-shaped elements following growth on ISP 3 agar after incubation at 28 °C for 10 days. Bar 1µm.

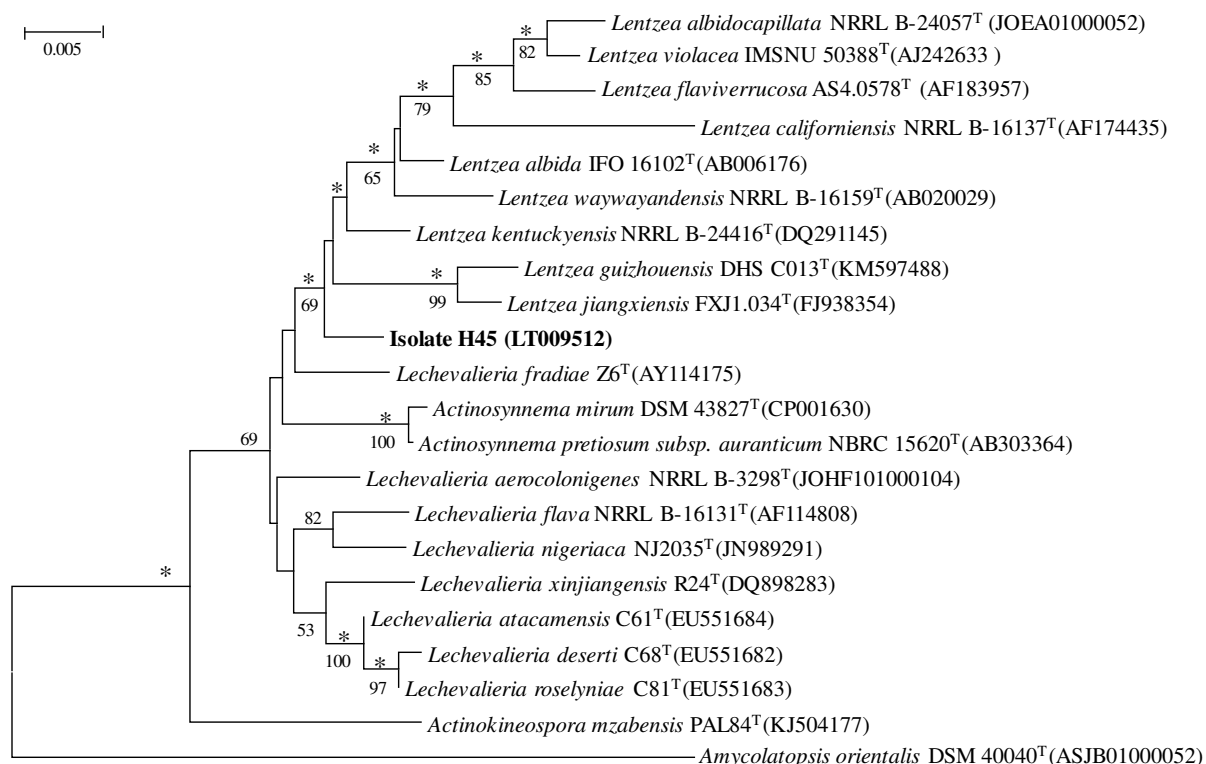


Figure 3. Neighbour-joining phylogenetic tree based on 16S rRNA gene sequences showing relationships between isolate H45 and the type strains of *Lentzea* and *Lechevalieria* species. Asterisks indicate branches of the tree that were also recovered using the maximum-likelihood and maximum-parsimony tree-making methods. Numbers at the nodes indicate levels of bootstrap support based on a neighbour-joining analysis of 1000 resampled datasets, only values above 50% are shown.

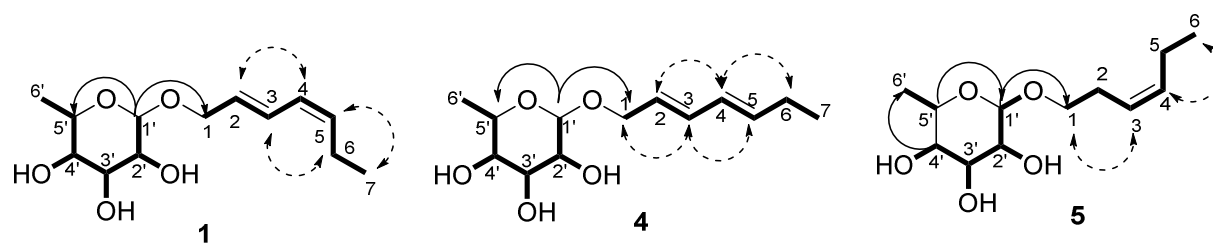


Figure 4. Key COSY (—), HMBC (↷) and ROESY (↘) correlations of compounds 1, 4, and 5.

1 **Table 1.** ^{13}C (150 MHz) NMR spectroscopic data for lentzeosides A–F (**1–6**) in $\text{DMSO-}d_6$

Position	1	2	3	4	5	6
	δC , mult.	δC , mult.	δC , mult.	δC , mult.	δC , mult.	δC , mult.
1	68.3, CH_2	66.5, CH_2	68.2, CH_2	68.3, CH_2	66.1, CH_2	68.2, CH_2
2	129.6, CH	129.5, CH	129.6, CH	127.1, CH	27.2, CH	27.6, CH
3	127.0, CH	127.2, CH	127.1, CH	132.5, CH	125.4, CH	125.2, CH
4	127.4, CH	127.3, CH	127.4, CH	128.5, CH	133.0, CH	132.9, CH
5	133.7, CH	133.9, CH	133.7, CH	136.5, CH	20.1, CH_2	20.1, CH_2
6	20.5, CH_2	20.5, CH_2	20.5, CH_2	25.0, CH_2	14.2, CH_3	14.2, CH_3
7	14.2, CH_3	14.1, CH_3	14.2, CH_3	13.4, CH_2		
1'	102.1, CH	99.3, CH	102.0, CH	99.1, CH	99.9, CH	102.7, CH
2'	73.7, CH	70.7, CH	73.5, CH	70.7, CH	70.7, CH	73.6, CH
3'	76.4, CH	70.5, CH	76.7, CH	70.5, CH	70.5, CH	76.5, CH
4'	75.3, CH	72.0, CH	68.2, CH	72.0, CH	72.0, CH	75.3, CH
5'	71.5, CH	68.5, CH	76.9, CH	68.5, CH	68.4, CH	71.5, CH
6'	17.9, CH_3	17.9, CH_3	61.1, CH_2	17.9, CH_3	17.9, CH_3	17.9, CH_3

2

3

4

5

6

7

8

9

10

1 **Table 2.** ^1H (600 MHz) NMR spectroscopic data for lentzeosides A–F (**1–6**) in $\text{DMSO-}d_6$

Position	1	2	3	4	5	6
	δ_{H} , mult. (J in Hz)	δ_{H} , mult. (J in Hz)	δ_{H} , mult. (J in Hz)	δ_{H} , mult. (J in Hz)	δ_{H} , mult. (J in Hz)	δ_{H} , mult. (J in Hz)
1	4.26 (dd, 13.2, 5.4)	4.11 (dd, 12.9, 5.3)	4.32 (dd, 13.7, 5.8)	4.06 (dd, 12.2, 5.3)	3.51 (m)	3.66 (m)
	4.08 (dd, 13.1, 5.2)	3.97 (dd, 12.7, 5.2)	4.10 (dd, 13.6, 6.5)	3.91 (dd, 12.4, 5.1)		3.42 (m)
2	5.71 (dt, 16.1, 6.3)	5.73 (dt, 15.9, 6.1)	5.73 (dt, 15.7, 5.9)	5.63 (dt, 16.1, 5.8)	2.24 (m)	2.26 (m)
3	6.58 (t, 14.5)	6.51 (t, 14.2)	6.59 (dd, 15.2, 11.2)	6.18 (t, 15.3)	5.32 (m)	5.33 (m)
4	5.94 (t, 11.2)	5.96 (t, 11.3)	5.96 (t, 11.1)	6.04 (t, 15.1)	5.42 (m)	5.42 (m)
5	5.42 (dt, 10.1, 6.7)	5.43 (dt, 10.5, 6.2)	5.42 (dt, 10.9, 6.5)	5.75 (dt, 15.5, 6.5)	2.01 (m)	2.01 (m)
6	2.16 (m)	2.16 (m)	2.16 (m)	2.07 (m)	0.92 (t, 7.6)	0.92 (t, 7.6)
7	0.94 (t, 7.5)	0.95 (t, 7.5)	0.94 (t, 7.5)	0.96 (t, 7.4)		
1'	4.15 (d, 7.8)	4.57 (br s)	4.15 (d, 7.9)	4.56 (br s)	4.54 (br s)	4.12 (d, 7.8)
2'	2.98 (t, 7.5)	3.41 (m)	2.97 (m)	3.40 (m)	3.39 (m)	2.94 (t, 7.9)
3'	3.09 (t, 8.6)	3.60 (br s)	3.12 (t, 7.6)	3.59 (br s)	3.57 (br s)	3.08 (t, 8.8)
4'	2.80 (t, 7.6)	3.18 (m)	3.04 (m)	3.17 (m)	3.17 (t, 8.9)	2.79 (t, 8.6)
5'	3.15 (m)	3.38 (m)	3.05 (m)	3.38 (m)	3.37 (m)	3.15 (m)
6'	1.15 (d, 6.1)	1.14 (d, 6.4)	3.66 (dd, 11.5, 5.6)	1.13 (d, 6.1)	1.12 (d, 6.3)	1.14 (d, 6.3)
			3.43 (m)			
OH-2'	5.07 (br s)		5.08 (d, 4.4)	4.74 (br s)	4.72 (br s)	4.91 (d, 18.1)
OH-3'	4.96 (br s)		4.91 (d, 3.9)		4.51 (br s)	4.94 (br s)
OH-4'	4.96 (br s)		4.96 (br s)	4.47 (br s)	4.70 (br s)	4.91 (br s)
OH-6'			4.49 (t, 5.7)			

2